Research Article

polymers advanced technologies

Received: 1 November 2009, Revised: 22 January 2010, Accepted: 25 January 2010, Published online in Wiley Online Library: 13 April 2010

(wileyonlinelibrary.com) DOI: 10.1002/pat.1690

Synthesis and thermal properties of antimony doped tin oxide/waterborne polyurethane nanocomposite films as heat insulating materials

Zhen Dai[a], Zhihua Li[a], Li Li[a] and Gewen Xu[a]*

The waterborne polyurethane (WPU) was synthesized from the polycondensation between isophorone diisocyanate (IPDI) and polyoxypropylene glycol (N-210) and then dispersed into water. Subsequently, the WPU emulsion was modified with antimony doped tin oxide (ATO) nanoparticle by ultrasonic dispersion. The ATO/WPU emulsion was cast onto Teflon molds. After being dried, ATO/WPU films were prepared. TEM indicated that the ATO nanoparticles were homogeneously dispersed in the polymer matrix at the nanometer scale. DSC showed that the ATO/WPU nanocomposites displayed increased glass transition temperatures compared to the control WPU. The mechanical properties of the films were characterized by dynamic-mechanical analysis (DMA). The higher glass transition temperature and storage modulus indicates the superior mechanical properties of WPU modified by ATO nanoparticles over the conventional unmodified WPU. The thermal behaviors of the films were evaluated by thermogravimetric analysis (TGA). It could be found that the incorporation of ATO into WPU can improve the thermal stability dramatically. The results from UV–visible–near infrared spectra indicated that the ATO/WPU films could decrease the infrared transmission effectively. The heat-insulation measurements showed that glass coated with ATO/WPU films possessed better heat-insulating effect than empty glass. Copyright © 2010 John Wiley & Sons, Ltd.

Keywords: waterborne polyurethane; ATO nanoparticles; heat insulating; modification

INTRODUCTION

With the improvement of economy and development of technology, environmental protection and energy conservation have been the focus of research and exploitation. The sunshine can pass the glass of the buildings so that the temperature inside the room is very high in summer. Thus, cooling the air will consume much energy by air conditioner. In recent years, method of the heat reflection membrane glass is used widely to insulate heat transmission. However, the non-transparency of heat reflection membrane glass in visible region greatly restricts its application. Consequently, transparent and heat insulating coatings have attracted great attention for their wide applications in low thermal conductivity, transparency, and simple construction technology.[1–4] The energy of solar radiation mainly concentrates in the wavelength range of 0.2–2.5 μm, and most of the energy distributes in infrared region. Therefore, preventing the transmission of infrared light can reach good insulating effect as well as transparency.[5–8]

Polyurethane coatings are widely used in various industrial fields because of its high tensile strength and modulus, low shrinkage on cure, high adhesion to many substrates, good weatherability and wearability.[9–13] As a promising "green" material, waterborne polyurethane (WPU) presents the attractive characteristics of non-toxicity, non-pollution, non-combustion, and competitive price. Recently, many academic and industrial researchers are devoted to study the modification of WPU, including grafting,[14] copolymerization,[15] and blending.[16] However, WPU coatings with transparent and heat-insulating effect are seldom reported.

Antimony doped tin oxide (ATO) is a well-known optically transparent, infrared light insulating and electrically conducting oxide.[17–20] If ATO nanoparticles are blended into WPU emulsion, a transparent WPU coating with excellent heat-insulating effect will be created and applied to glass. Based on this idea, WPU coating modified by mixing ATO nanoparticles into WPU emulsion was prepared and then coating them on glass slides in this paper. The mechanical and thermal properties of resulted films were characterized by dynamic-mechanical analysis (DMA), thermogravimetric analysis (TGA), UV–visible–near infrared (UV–Vis–NIR) spectrophotometer, and heat-insulation effect measurements.

EXPERIMENTAL

Materials

Isophorone diisocyanate (IPDI) was industrial grade and supplied by Mitsui Chemicals, Inc. Polyoxypropylene glycol (N-210) was industrial grade and provided by Nanjing Jingling Chemical

* *Correspondence to: G. Xu, Anhui Key Laboratory of Environment-Friendly Polymer Materials, School of Chemistry and Chemical Engineering, Anhui University, Hefei 230039, Anhui Province, P.R. China.*
E-mail: gwxu@ahu.edu.cn

a *Z. Dai, Z. Li, L. Li, G. Xu*
School of Chemistry and Chemical Engineering, Anhui University, Hefei 230039, Anhui Province, P.R. China

Industry Co. Ltd. (molecular weight = 1000 g/mol). Dimethyopropionic acid (DMPA) was industrial grade and provided by Perstop Chemicals Company. Diethylene glycol (DEG) was reagent grade and purchased from Shanghai Chemical No. 3 factory. Trimethylolpropane (TMP) was supplied by Nanjing Huahong Chemical Industry Co. Ltd. The pH buffer AMP-95 was supplied by DOW-ANGUS and used as received. Ethylenediamine (EDA), triethylamine (TEA), and ammonium hydroxide from Shanghai Ningxin chemical reagent factory were all reagent grade and were used as received. ATO nanoparticles solution modified by surfactant (solid content: 50%) was provided by Huzheng Nanotechonolgy Co. Ltd. and used without any further purification. Acetone was reagent grade and purchased from Sinopharm Chemical Reagent Co. Ltd.

Synthesis

Preparation of waterborne polyurethane emulsion

IPDI (33.3 g) and 30.6 g of N-210 were charged into a three-neck and round-bottom 250 ml glass flask equipped with a thermometer, a reflux condenser, and a mechanical stirrer. The mixture was stirred vigorously and heated to 90°C for about 2 hr. The reaction mixture was cooled to 60°C, and then 2.40 g of DMPA, 6.36 g of DEG, 0.67 g of TMP were introduced into the flask. The reaction was kept at 60°C for 5 hr. After cooling to room temperature, 2.64 ml of TEA, 3.57 g of EDA, and 150 ml of deionized water were added into the polyurethane and dispersed for 20 min. The solvent of acetone was removed by vacuum distillation and then the white emulsion was obtained. The synthetic route of ATO/WPU emulsions was shown in Scheme 1.

Preparation of ATO/WPU emulsion

Above WPU emulsion (30.0 g) was added into container and adjusted its pH value using the pH buffer AMP-95. Afterwards, 1 wt% ATO nanoparticles as total weight were mixed into the WPU emulsion. The mixture was dispersed for 20 min by ultrasonic dispersion. Then the WPU emulsion modified by ATO nanoparticle was obtained. Other samples were synthesized in the same procedures. The composition and average particle size of the ATO/WPU emulsions were listed in Table 1.

Preparation of ATO/WPU films

The ATO/WPU emulsion was cast onto Teflon molds. After natural drying for 2 days, ATO/WPU films were prepared. Meanwhile, the ATO/WPU emulsion was coated on the surface of glass (specimen: $10 \times 10\,mm^2$) using blade coater (type: QTG, blade thickness: 125 μm). The glass with ATO/WPU coatings was placed horizontally at the room temperature for 2 days and then dried in the oven at 80°C for 4 hr.

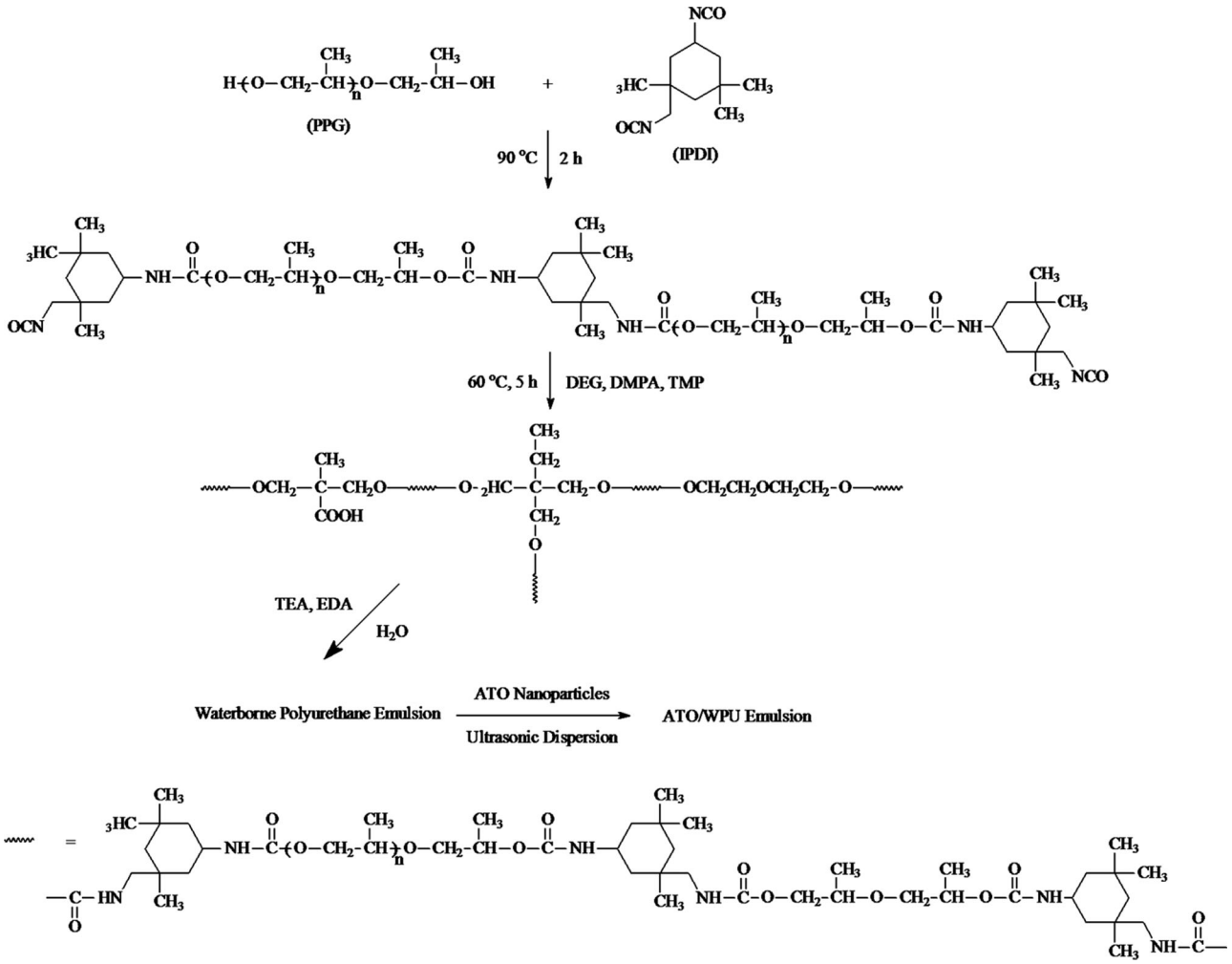

Scheme 1. Synthetic route of ATO/WPU dispersion.

Table 1. The composition and average particle size of ATO/WPU emulsions

Sample code	WPU content (g)	ATO content (g)	Average particle size (nm)
WPU	30.0	0	65.60
WPU-1	30.0	0.6	64.98
WPU-2	30.0	1.8	62.48
WPU-3	30.0	3.0	64.98
WPU-4	30.0	4.2	80.33

Measurements

Mechanical properties test

The mechanical behaviors of ATO/WPU films were measured by CMT6104 computer controlled universal tensile testing machine according to GB/T 17200-1997. The specimens used for the test were of dimensions $30 \times 3 \times 1\ mm^3$.

Thermogravimetric analysis (TGA)

The TGA of samples was carried out with Q5000 thermal analyzer (TA Co., USA) from 50 to 700°C at a heating rate of 20 °C/min in air atmosphere (flow rate of 100 ml/min).

Differential scanning calorimetry (DSC)

The differential scanning calorimetry (DSC) measurements were performed using a Perkin Elmer differential scanning calorimeter which was calibrated according to the standard procedure using a heating rate of 10°C/min.

Dynamic-mechanical analyses (DMA)

DMAs were performed with the Rheometric Q800 DMA (Apparatus, USA) from −100 to 200°C at a heating rate of 3°C/min, at a frequency of 1 Hz in the tensile configuration. The specimens used for the test were of dimensions $20 \times 5 \times 1\ mm^3$.

Attenuated total reflection Fourier transform infrared (ATR-FTIR)

The ATR-FTIR spectra were recorded using a Nicolet 6700 spectrophotometer equipped with a total reflection device. The wavenumber range was set from 4000 to 650 cm^{-1}.

Transmission electron microscopy (TEM)

TEM was performed on a JEOL JEM-2100 high-resolution transmission electron microscope at an acceleration voltage of 200 kV.

UV–Vis–NIR spectrophotometer

UV–Vis–NIR spectrophotometer (HITACHI, U-4100) was employed to characterize the transmittance of the glass with the ATO/WPU coatings. The transition mode was used and the wavenumber range was set from 2500 to 250 cm^{-1}.

Heat-insulation effect test

The heat-insulation effect measurement was designed as shown in Fig. 1. Temperature from four thermometers was recorded every 5 min.

RESULTS AND DISCUSSION

Determination chemical structures of WPU and ATO/WPU film by ATR-FTIR

The ATR-FTIR spectra of WPU and WPU-4 film are given in Fig. 2. The assignment of ATR-FTIR spectra of WPU film is listed in Table 2. The ATR-FTIR spectrum of WPU film possesses several

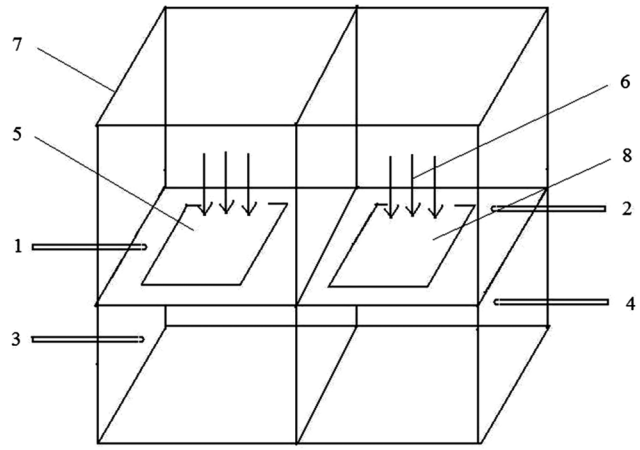

1,2,3,4-**Thermometer**; **5-Glass with ATO/WPU coating**; 6-**Infrared light**; 7-**Heat insulation box**; 8-**Glass**.

Figure 1. Diagram illustrating the experimental box for heat insulating measurement.

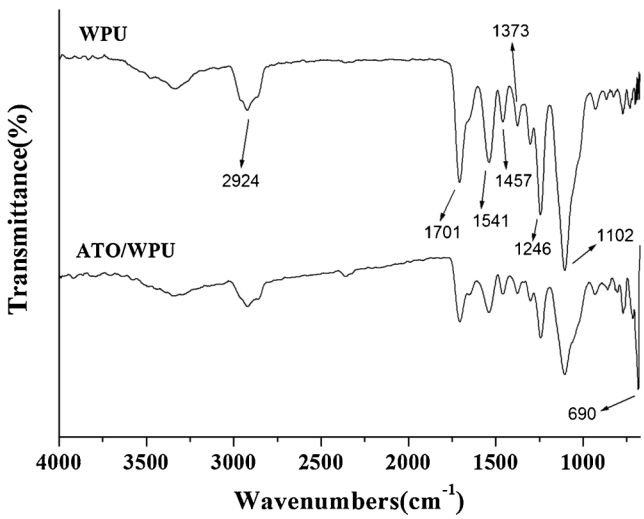

Figure 2. FTIR spectra of WPU and ATO/WPU films.

Table 2. Assignment of ATR-FTIR Spectra of WPU and ATO/WPU films

Wavenumber (cm^{-1})	Assignment
WPU	
2924	$-CH_3$ and $-CH_2-$ stretching vibration
1701	Carbonyl stretching vibration
1541	N–H stretching vibration
1457, 1373	Asymmetric and symmetric $-CH_3$ deformation vibration
1246	C–O–C stretching vibration of ester
1102	C–O–C stretching vibration of ether
ATO/WPU	
2924	$-CH_3$ and $-CH_2-$ stretching vibration
1701	Carbonyl stretching vibrations
1541	N–H stretching vibration
1457, 1373	Asymmetric and symmetric $-CH_3$ deformation vibration
1246	C–O–C stretching vibration of ester
1102	C–O–C stretching vibration of ether
690	Sn–O stretching vibration of ATO

characteristic absorption bands: the broad bands at around 2924 cm^{-1} due to $-CH_3$ and $-CH_2-$ stretching vibration; the strong absorption bands at 1701 cm^{-1} corresponded to carbonyl stretching vibrations of the polyurethane backbone and the bands at 1457 and 1373 cm^{-1} corresponded to asymmetric and symmetric $-CH_3$ deformation vibration; the absorption bands at 1541 cm^{-1} assigned to N–H stretching vibration; the bands at 1246 cm^{-1} assigned to C–O–C stretching vibration of ester; the strong bands at 1102 cm^{-1} assigned to C–O–C stretching vibration of ether.[21] Moreover, it can be seen from Fig. 2 that the ATR-FTIR spectra of WPU-4 film show all the above characteristic absorption bands of WPU film. It is worth noting that the new bands at 690 cm^{-1} of the ATR-FTIR spectra of WPU-4 film are due to Sn–O stretching vibration of ATO.

Morphology of ATO/WPU hybirds

The TEM are employed to observe the morphology of the ATO/WPU hybirds. Figure 3 representatively displays the TEM micrographs of ATO/WPU hybird containing 7 wt% of ATO. As can be seen, the white dots are polyurethane matrix and the black dots are ATO nanoparticles. The result suggests that the ATO nanoparticles form uniform clusters of particles and are homogeneously dispersed in the polymer matrix without agglomeration. The similar phenomenon have been reported by the earlier literiture.[22]

Glass transition behavior

The glass transition temperatures of ATO/WPU hybird films are measured by DSC, as shown in Fig. 4. The control WPU displays a glass transition at 20.2°C, indicating that this material can be used as elastomer. For the ATO/WPU hybird films, all of the DSC curves exhibit single glass transition temperatures (T_g) in the

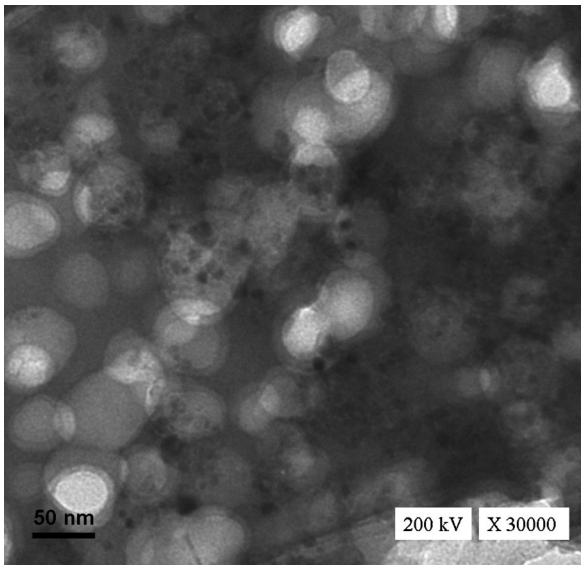

Figure 3. TEM micrograph of the ATO/WPU hybird with 7 wt% ATO.

experimental temperature range (from −60 to 160°C). In comparison with the control WPU, the ATO/WPU hybrids show an enhanced T_g, which increases with increasing ATO content. In ATO/WPU hybrid films, the increase in the glass transition temperature is generally interpreted on the basis of nanoreinforcement of the ATO nanoparticles in the polymer matrices, which is able to restrict the motions of the macromolecular chains.[23–25] In the present case, the T_g enhancement is not only ascribed to the nanoreinforcement of the ATO nanoparticles but also attributed to the enhancement of the cross-linking density of the WPU networks.

Mechanical properties of ATO/WPU films

The effect of the addition amount of ATO on the mechanical properties of ATO/WPU films are studied using the computer controlled universal tensile testing machine. Table 3 presents the mechanical properties of WPU films with different contents of ATO. For the pure WPU film, the tensile strength is about

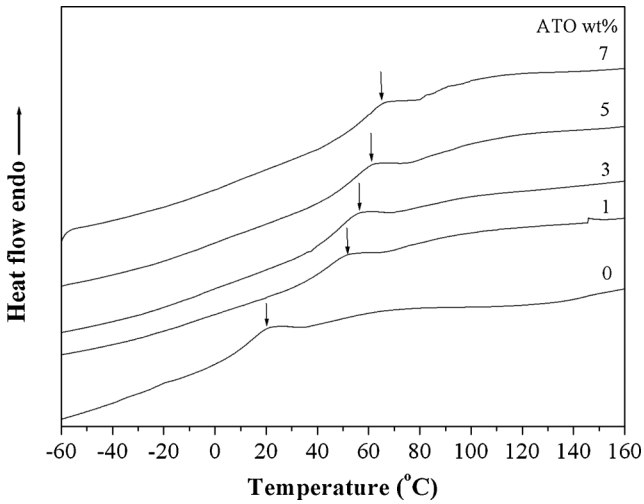

Figure 4. DSC curves of WPU and ATO/WPU films.

Table 3. Mechanical properties of WPU films with different contents of ATO

Sample	Strength intensity (MPa)	Elongation at break (%)
WPU	9.05	679.9
WPU-1	18	785.7
WPU-2	19.87	678.44
WPU-3	18.48	658.16
WPU-4	18.08	561.87

9.05 MPa and the elongation at break is more than 670%. The incorporation of ATO nanoparticles gives nanoreinforcement impact on the WPU firstly, but the tensile strength of ATO/WPU hybird films begins to decrease at high ATO load. The elongation at break of ATO/WPU films shows the same trend as the addition amount of ATO increases. The increased cross-link density could be responsible for the decrease in the elongation at break of the materials.

Dynamic mechanical analysis (DMA)

Viscoelastic property of ATO/WPU films are evaluated by DMA. The tan δ versus temperature for WPU and ATO/WPU films are plotted in Fig. 5. The glass transition temperature (T_g) is also obtained from the peak of tan δ curve. The T_g of WPU is found to be 24.9°C while WPU-1, WPU-2, WPU-3, and WPU-4 individually show single peak at 78.9, 80.3, 80.4, and 81.0°C, respectively. This suggests that increasing ATO content has a favorable influence on T_g values of the hybrid coatings. The results are consistent with DSC measurement.

The storage modulus of the ATO/WPU nanocomposite films with different ATO contents as a function of temperature are plotted in Fig. 6. As can be seen, the initial storage modulus of WPU is 7.57×10^8 Pa, whereas those of WPU-1, WPU-2, WPU-3, and WPU-4 are 4.36×10^9, 4.72×10^9, 4.83×10^9, and 5.99×10^9 Pa, respectively. The introduction of ATO gives a positive impact on the storage modulus of WPU films. This

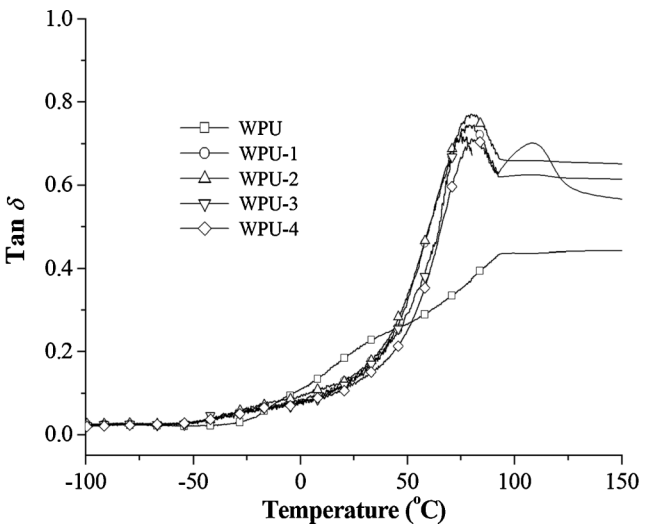

Figure 5. DMA tan δ curves of WPU and ATO/WPU films.

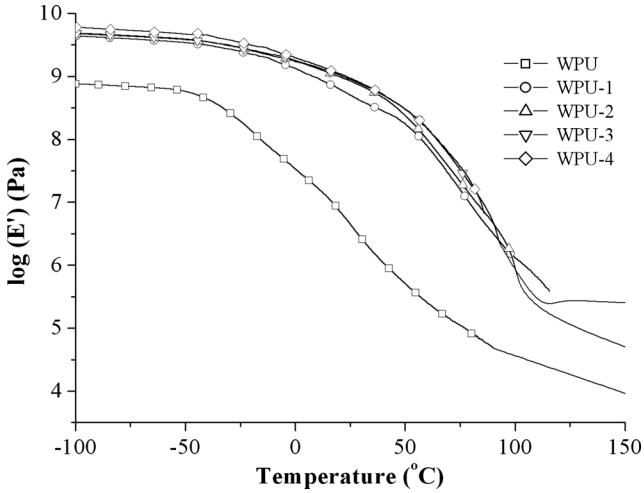

Figure 6. DMA storage modulus curves of WPU and ATO/WPU films.

phenomenon may be explained as follows: for polymer nanocomposites, the storage modulus depends on the inorganic phase, the interfacial interaction and the cross-linking density of the polymer matrix. Generally, an introduction of inorganic nanoparticles leads to an enhancement of storage modulus, and the interfacial interaction does not deteriorate the storage modulus, even though it is poor.[26] Therefore, a improvement of the cross-linking density of the WPU matrix could presumably be responsible for the enhanced storage modulus of the ATO/WPU nanocomposites.

Thermal properties of ATO/WPU films

TGA is one of the most widely used tools for rapid evaluation of the thermal stability of various polymers. The TG and DTG curves of WPU and ATO/WPU films in air atmosphere are shown in Fig. 7a,b. The onset degradation temperature (T_d) of samples which is evaluated by the temperature of 10 wt% weight loss ($T_{-10\%}$), the mid-point temperature of the degradation ($T_{-50\%}$), and the solid residue at 700°C are obtained from the TG curves; the temperature of the maximum weight loss rate (T_{max}) of samples is obtained from the DTG curves. These data are listed in Table 4.

The thermal oxidative degradation process of the WPU film has one stage in the temperature ranges of 250–350°C corresponding to T_{max} of 278.8°C. The solid residue at 700°C is 1.87%. The weight loss below 200°C is mainly due to small molecular evolution products, such as water or unreacted monomer. The thermal degradation from 250 to 350°C is the main decomposition process. Some complex chemical reactions occur at this stage, including the chain scission of the WPU backbone. It can be seen from Fig. 5 that the incorporation of ATO into WPU obviously improves the onset decomposition temperatures (T_d) of ATO/WPU films than pure WPU. The T_d increases gradually from 256.1 to 265.1°C with the increase of ATO addition. The $T_{-50\%}$ of WPU-4 is 26°C higher than that of WPU. As the addition amount of ATO increases, the char residue at 700°C also increases gradually. Moreover, WPU-4 after the decomposition at 700°C left about 18.31% residue, whereas the residue for pure WPU at this temperature is 1.87%. From Fig. 5b, it can be found that the temperature of the maximum weight loss rate (T_{max}) is improved

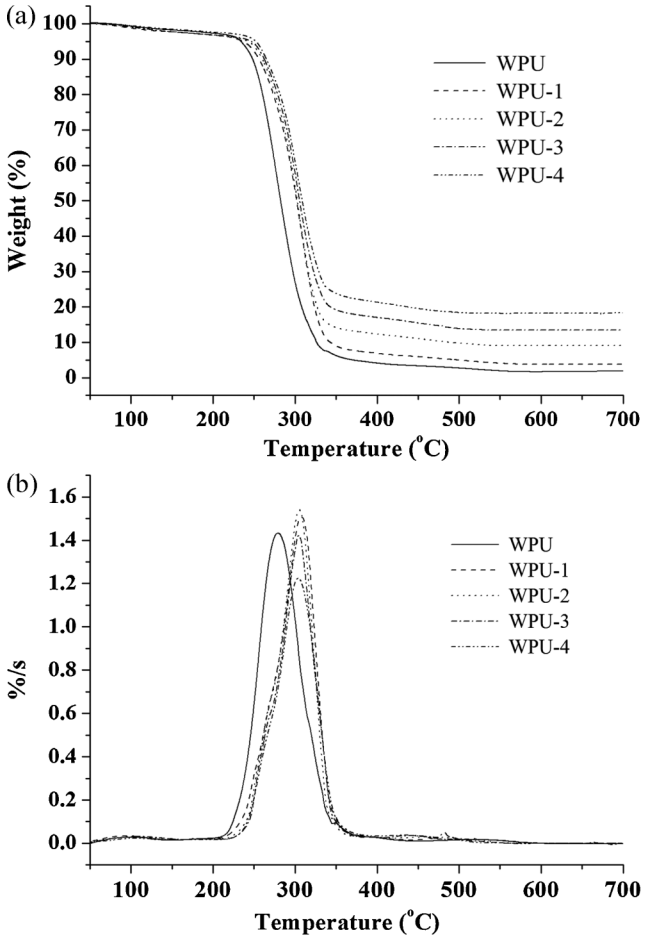

Figure 7. (a) TG and (b) DTG curves of WPU, WPU-1, WPU-2, WPU-3, and WPU-4 in air atmosphere.

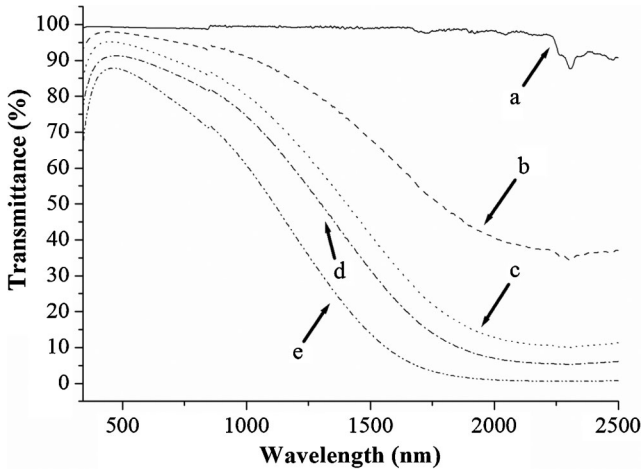

Figure 8. The optical transmittance spectra of (a) WPU on glass, (b) WPU-1 on glass, (c) WPU-2 on glass, (d) WPU-3 on glass, and (e) WPU-4 on glass.

because of the addition of ATO. From above all, it can be concluded that the incorporation of ATO into WPU can improve the thermal stability dramatically.

UV–Vis–NIR spectrophotometer analysis

The optical properties of ATO/WPU hybird films are evaluated by UV–Vis–NIR spectra.[27,28] Fig. 8 shows the transmittance spectra as a function of wavelength in the wavelength range 350–2500 nm for WPU and ATO/WPU thin film samples, prepared on glass substrate. The spectra show that the glass coated with WPU films has high transmittance in both visible region and near infrared region. However, the glasses coated with ATO/WPU films have a sharp fall of transmittance at the near infrared region. Moreover, as the addition amount of ATO increases, the transmittance of the ATO/WPU films on the glasses decreases gradually. The transmittance of WPU-4 thin film deposited on glass substrate is as low as 0.63% in the wavelength range 2000–2500 nm, whereas its transmittance at the visible region is nearly 80.0%. This means ATO/WPU films can prevent most of infrared light passing the glass. In addition to this, the decrease of average transmittance in the visible wavelength region is also observed for ATO/WPU films. In the visible wavelength range the lowest average transmittance of 75% has been observed for WPU-4 films deposited on glass substrate.

Heat insulating test of ATO/WPU films

The heat insulating effect of ATO/WPU films is investigated by self-made heat insulating box. Temperature recorded from four thermometers is presented in Fig. 9. It can be observed that as the ATO addition content increases, the temperature of the room over the glass increases while that of the room lower the glass decreases. The temperature difference of the rooms over and under the glass coated with ATO/WPU films increases obviously, compared to that of the glass without ATO/WPU films. This means ATO/WPU films can prevent heat transmission and heat diffusion effectively.

Table 4. TG Data of WPU and ATO/WPU films in air

Samples	$T_{-10\%}$ (°C)	$T_{-50\%}$ (°C)	T_{max} (°C)	Char residue (%) at 700°C
WPU	248.3	282.4	278.8	1.87
WPU-1	256.1	302.0	308.0	3.83
WPU-2	260.2	302.7	305.3	9.14
WPU-3	262.5	305.6	304.8	13.52
WPU-4	265.1	308.8	303.9	18.31

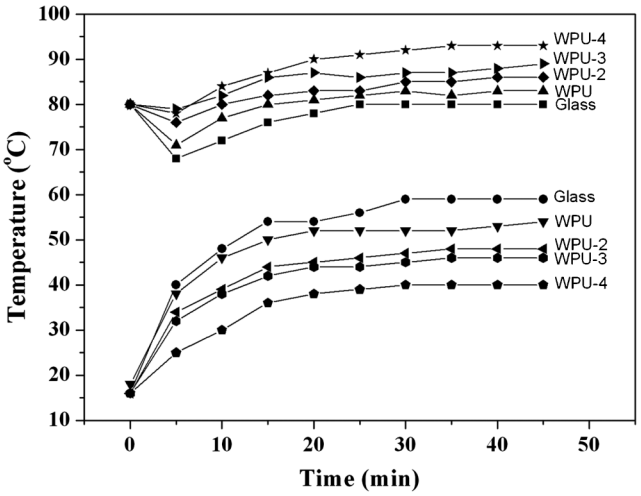

Figure 9. Heat-insulation effect measurement of empty glass and glass coated with WPU and ATO/WPU films.

CONCLUSIONS

A series of ATO/WPU nanocomposite films containing 0, 1, 3, 5, and 7 wt% content of ATO were prepared. TEM suggested that ATO nanoparticles formed uniform clusters of particles and were homogeneously dispersed in the polymer matrix without agglomeration. DSC showed that the ATO/WPU nanocomposites displayed increased glass transition temperatures compared to the control WPU. The incorporation of ATO into WPU can increase the mechanical properties of WPU. TGA thermogram indicated that the introduction of ATO provided higher T_d, T_{max} and the char residue to WPU. The viscoelastic properties of the films were characterized by DMA. It was found that WPU films modified by ATO nanoparticles exhibited higher glass transition temperature and storage modulus than the conventional unmodified WPU. The results from UV–Vis–NIR spectra indicated that the ATO/WPU films could decrease the infrared transmission effectively. The ATO/WPU films, possessing good mechanical properties and thermal stability and excellent heat insulating effect, were expected to be widely applied as a promising heat insulating material.

REFERENCES

[1] J. M. Ni, Q. N. Zhao, X. J. Zhao, *Prog. Org. Coat.* **2009**, *64*, 317–321.
[2] S. W. Kim, D. K. Lee, Y. S. Kang, Y. J. Kim, *Mol. Cryst. Liq. Cryst.* **2006**, *445*, 81–92.
[3] M. Modesti, A. Lorenzetti, S. Besco, *Polym. Eng. Sci.* **2007**, *47*, 1351–1358.
[4] Y. H. Kim, S. J. Choi, A. M. Kim, M. S. Han, W. N. Kim, K. T. Bang, *Macromol. Res.* **2007**, *15*, 676–681.
[5] R. F. Brady, L. V. Wake, *Prog. Org. Coat.* **1992**, *20*, 1–25.
[6] S. Heinz, S. Uwe, K. Wilfried, H. Bodo, US Patent 6,306,525, October 23, **2001**.
[7] G. Hans, H. Bernhard, S. Heinz, US Patent 5,837,361, November 17, **1998**.
[8] K. Tetsuo, US Patent 4,483,899, November 20, **1984**.
[9] J. J. Chen, C. F. Zhu, H. T. Deng, Z. N. Qin, Y. Q. Bai, *J. Polym. Res.* **2009**, *16*, 375–380.
[10] X. L. Chen, Y. Hu, L. Song, C. Jiao, *Polym. Adv. Technol.* **2008**, *19*, 322–327.
[11] C. X. Zhao, W. D. Zhang, D. C. Sun, *Polym. Compos.* **2009**, *30*, 649–654.
[12] C. Y. Bai, X. Y. Zhang, J. B. Dai, C. Y. Zhang, *Prog. Org. Coat.* **2007**, *59*, 331–336.
[13] A. Asif, L. H. Hu, W. F. Shi, *Colloid Polym. Sci.* **2009**, *287*, 1041–1049.
[14] A. Asif, W. F. Shi, *Polym. Adv. Technol.* **2004**, *15*, 669–675.
[15] H. Du, Y. H. Zhao, N. Yin, Q. F. Li, J. W. Wang, M. Q. Kang, H. W. Xiang, X. K. Wang, *J. Appl. Polym. Sci.* **2008**, *110*, 3156–3161.
[16] H. X. Pan, D. J. Chen, *Eur. Polym. J.* **2007**, *43*, 3766–3772.
[17] K. Ravichandran, P. Philominathan, *Mater. Lett.* **2008**, *62*, 2980–2983.
[18] R. Outemzabet, N. Bouras, N. Kesri, *Thin Solid Films* **2007**, *515*, 6518–6520.
[19] T. R. Giraldi, M. T. Escote, A. P. Maciel, E. Longo, E. R. Leite, J. A. Varela, *Thin Solid Films* **2006**, *515*, 2678–2685.
[20] D. L. Zhang, L. Tao, Z. B. Deng, J. B. Zhang, L. Y. Chen, *Mater. Chem. Phys.* **2006**, *100*, 275–280.
[21] J. H. Wang, X. Y. Zhang, J. B. Dai, *Chin. J. Anal. Chem.* **2007**, *35*, 964–968.
[22] J. Feng, B. Y. Huang, M. Q. Zhong, *J. Colloid Interface Sci.* **2009**, *336*, 268–272.
[23] A. Lee, J. D. Lichtenhan, *Macromolecules* **1998**, *31*, 4970–4974.
[24] P. T. Mather, H. G. Jeon, A. Romo-Uribe, T. S. Haddad, J. D. Lichtenhan, *Macromolecules* **1999**, *32*, 1194–1203.
[25] Y. H. Liu, Y. Ni, S. X. Zheng, *Macromol. Chem. Phys.* **2006**, *207*, 1842–1851.
[26] S. X. Zhou, L. M. Wu, *Macromol. Chem. Phys.* **2008**, *209*, 1170–1181.
[27] H. Bisht, H. T. Eun, A. Mehrtens, M. A. Aegerter, *Thin Solid Films* **1999**, *351*, 109–114.
[28] K. Ravichandran, P. Philominathan, *Mater. Lett.* **2008**, *62*, 2980–2983.

